

**END-TO-END TESTING OF THE LEKSELL GAMMA KNIFE ICON
SYSTEM**

A Thesis
Presented to
The Academic Faculty

by

Krista R. Burton

In Partial Fulfillment
of the Requirements for the Degree
Master of Science in Medical Physics

Georgia Institute of Technology
December 2017

COPYRIGHT © 2017 BY KRISTA R. BURTON

END-TO-END TESTING OF THE LEKSELL GAMMA KNIFE ICON SYSTEM

Approved by:

Dr. Chris Wang, Committee Chair, Co-Advisor
School of Mechanical Engineering
Georgia Institute of Technology

Sara Rahnema M.S., DABR, Co-Advisor
Medical Physicist
Emory Saint Joseph's Hospital

Dr. Nolan Hertel
School of Mechanical Engineering
Georgia Institute of Technology

Date Approved: December 5, 2017

ACKNOWLEDGEMENTS

First, I would like to thank God for blessing me with this gift and for affording me this opportunity at success. I would like to thank my parents for believing in my dreams and supporting me throughout my academic career. Additionally, I would like to thank Dr. Chris Wang, Sara Rahnema, and Matthew Giles for their constant guidance, support, and encouragement.

TABLE OF CONTENTS

ACKNOWLEDGEMENTS	iii
LIST OF TABLES	vi
LIST OF FIGURES	vii
LIST OF SYMBOLS AND ABBREVIATIONS	ix
SUMMARY	xi
CHAPTER 1. Introduction and Purpose	1
CHAPTER 2. BACKGROUND	3
CHAPTER 3. METHODS AND DESIGN	5
3.1 Overview.....	5
3.2 Leksell Gamma Knife Icon System.....	6
3.2.1 Cone Beam Computed Tomography.....	6
3.2.2 Infrared Motion Management (IFMM) System	8
3.3 Patient Workflow for Frameless Treatment	11
3.4 Lucy 3D QA Phantom	12
3.5 Phantom-Platform Device.....	14
3.5.1 Platform Design	14
3.5.2 Platform Motion Geometry	18
3.6 Leksell GammaPlan	20
3.7 End-to-End Testing Procedure.....	22
3.7.1 Platform Setup.....	22
3.7.2 Limitation of the Treatment Plan	26

3.7.3 CBCT and IFMM Evaluation.....	27
3.8 GAFChromic EBT3 Dosimetry Film	29
3.8.1 Optical Density.....	29
3.8.2 Film Calibration	31
3.8.3 Absolute Dose Calibration Curve	34
CHAPTER 4. Results and Discussion	37
4.1. Experimental vs. Measured Levels of Motion.....	37
4.2. Absolute Dose Measurements.....	40
4.2.1 Absolute Dose Curves.....	40
4.2.2 Dose Coverage for a Moving Target.....	50
4.2.3 Plot Statistics	52
CHAPTER 5. Conclusion	55
REFERENCES.....	58

LIST OF TABLES

Table 1	Experimental (at the nose) and measured (at the center) values of the level of motion achieved by the platform in the vertical direction	39
Table 2	Experimental (at the nose) and measured (at the center) values of the level of motion achieved by the platform in the horizontal direction	39
Table 3	Plot statistics corresponding to the absolute dose curves in Figures 14-18 for target films irradiated with constant <u>vertical</u> motion, compared to the reference film with no motion	53
Table 4	Plot statistics corresponding to the absolute dose curves in Figures 19-23 for target films irradiated with constant <u>horizontal</u> motion, compared to the reference film with no motion	54

LIST OF FIGURES

Figure 1	Front view of the Leksell Gamma Knife Icon system with C-arm attachment upright in the parked position	7
Figure 2	The infrared motion management (IFMM) system with highlighted tracking paths from the infrared camera to the reference markers on the nose of the patient and in the mask adapter	9
Figure 3	Patient in the mask adapter with nose marker and thermoplastic mask	9
Figure 4	Lucy 3D QA phantom mounted onto the precision leveling and rotational alignment base	13
Figure 5	Lucy 3D QA phantom design with spherical dimensions in mm	13
Figure 6	Drawing of the phantom platform device (overhead view) with dimensions given in inches	15
Figure 7	Offset cranks that determined the levels of motion for the device	17
Figure 8	Effects of the platform-phantom geometry on the level of motion allowed at the centered film and at the nose of the phantom	19
Figure 9	Structure of GAFChromic EBT3 Dosimetry Film	20
Figure 10	The Lucy phantom attached to the platform device in the mask adapter, with nose marker and non-reflective surface coverings	23
Figure 11	Overhead view of the film cassette insert inside of the Lucy phantom	25
Figure 12	Overhead view of the phantom-platform device holding Lucy in an orientation mimicking the head of a patient during treatment	26
Figure 13	The absolute calibration curve for the GAFChromic EBT3 film from lot number 05011701, where the Dose is given in Gy	36
Figure 14	Absolute dose curves in the vertical (l) and horizontal (r) profiles of Film 1, which had 0.5 mm vertical motion as observed by the IFMM, compared to the reference film with no motion.	44
Figure 15	Absolute dose curves in the vertical (l) and horizontal (r) profiles of Film 2, which had 1.5 mm vertical motion as observed by the	44

IFMM, compared to the reference film with no motion.

Figure 16	Absolute dose curves in the vertical (l) and horizontal (r) profiles of Film 3, which had 2.0 mm vertical motion as observed by the IFMM, compared to the reference film with no motion.	45
Figure 17	Absolute dose curves in the vertical (l) and horizontal (r) profiles of Film 4, which had 3.4 mm of vertical motion as observed by the IFMM, compared to the reference film with no motion.	45
Figure 18	Absolute dose curves in the vertical (l) and horizontal (r) profiles of Film 5, which had 4.0 mm of vertical motion as observed by the IFMM, compared to the reference film with no motion.	46
Figure 19	Absolute dose curves in the vertical (l) and horizontal (r) profiles of Film 6, which had 0.3 mm of horizontal motion as observed by the IFMM, compared to the reference film with no motion.	47
Figure 20	Absolute dose curves in the vertical (l) and horizontal (r) profiles of Film 7, which had 1.3 mm of horizontal motion as observed by the IFMM, compared to the reference film with no motion.	47
Figure 21	Absolute dose curves in the vertical (l) and horizontal (r) profiles of Film 8, which had 1.7 mm of horizontal motion as observed by the IFMM, compared to the reference film with no motion.	48
Figure 22	Absolute dose curves in the vertical (l) and horizontal (r) profiles of Film 9, which had 3.2 mm of horizontal motion as observed by the IFMM, compared to the reference film with no motion.	48
Figure 23	Absolute dose curves in the vertical (l) and horizontal (r) profiles of Film 10, which had 5.3 mm of horizontal motion as observed by the IFMM, compared to the reference film with no motion.	49

LIST OF SYMBOLS AND ABBREVIATIONS

2D	Two -Dimensional
3D	Three-Dimensional
AAPM	American Association of Physicists in Medicine
AI	Angiogram Imaging
cGy	Centi-Gray
cm	Centimeter
CT	Computed Tomography
CBCT	Cone-Beam Computed Tomography
CBCT _m	Cone-Beam Computed Tomography Image at Maximum Point in Range
CBCT _t	Cone-Beam Computed Tomography Treatment Image
dpi	Dots per Inch
FWHM	Full-Width Half Maximum
GK	Gamma Knife
GUI	Graphic User Interface
Gy	Gray
HDMM	High Definition Motion Management
IMRT	Image-Modulated Radiation Therapy
IF	Infrared
IFMM	Intra-Fraction Motion Management
KERMA	Kinetic Energy Released per unit Mass
keV	Kilo-Electron Volt
MR	Magnetic Resonance

MeV Mega-Electron Volt
mm Millimeter
OD Optical Density
PET Positron Emission Tomography
QA Quality Assurance
RIT Radiation Imaging Technology
SRS Stereotactic Radiosurgery
TG Task Group
VMAT Volumetric Arc Therapy

SUMMARY

The Leksell Gamma Knife Icon is a stereotactic radiosurgery system that is used to non-invasively treat brain lesions. It incorporates 192 fixed cobalt-60 sources, which ensures the highest degree of accuracy during treatment due to the minimization of potential error from stationary sources. The gamma knife's precision and special modifications for conformity to the human brain ensure faster treatments and fractionated options, delivered in a few hours on a single day, as opposed to treatment on consecutive days.

A titanium-alloy frame affixed to the skull of a patient before each treatment has defined the stereotactic coordinate system of previous gamma knife models, as well as provided complete patient immobilization during treatment. However, the newest gamma knife model from Elekta, the Icon, introduced a frameless treatment option that utilizes an on-board cone-beam computed tomography (CBCT) imager for patient positioning and a motion tracking system to monitor patient movement during treatment. When using this option, the stereotactic coordinate system is defined by the CT image taken before treatment, and a thermoplastic mask is used for moderate patient immobilization, as opposed to the titanium-alloy frame. Since the opportunities for positioning misalignment and out-of-tolerance patient movement is now introduced to the treatment, thorough research and end-to-end testing was conducted to make sure that correction calculations and monitoring methods are being performed to keep these concerns to a minimum and provide an accurate and precise radiosurgery procedure.

This project was conducted to consider extreme patient movement during radiosurgery procedures and provide additional end-to-end testing on the Leksell Gamma Knife system at Emory Saint Joseph's Hospital in Atlanta, Georgia. The performed testing verified the integrated imaging system by treating a moving target that required position shifts between treatments to mimic patient misalignments, observing the ability of the system to accurately correct patient shifts during setup. Additionally, this work evaluated the motion tracking system by treating a moving target, which mimicked patient chin-like movements during treatment, monitoring the tolerance at which there was a clinical detriment to the quality of the plan due to patient motion.

CHAPTER 1. INTRODUCTION AND PURPOSE

The Leksell Gamma Knife Icon is a stereotactic radiosurgery system that is used to non-invasively treat brain conditions. It incorporates 192 fixed Cobalt-60 sources separated into eight independently moveable sectors. This design ensures the highest degree of accuracy during treatment due to the stationary sources minimizing potential error from motion [6]. The system also includes three collimator sizes (4, 8, and 16 mm), which allows for different size radiation shots that offer the ability to create complex treatment plans for high conformity to the intracranial structure being treated. The Gamma Knife (GK) renders a partial-hemisphere equipment geometry that is designed specifically for the human brain to ensure faster, more accurate treatments, which now includes a frameless option that can be delivered in a few hours on a single day, as opposed to treatment on consecutive days as with conventional linear accelerator methods.

Prior to the Icon system, previous GK models utilized a titanium-alloy frame, the Leksell Coordinate Frame G, which was affixed to the skull of a patient prior to imaging and treatment. This frame defined the stereotactic coordinate system that specified the exact position of the treatment area relative to the frame, as well as provided complete patient immobilization during treatment. However, the newer Icon system not only offers the frame option but also introduces a frameless treatment option that utilizes an on-board cone-beam computed tomography (CBCT) imager for patient positioning and the intra-fraction motion management (IFMM) system to monitor the patient's movements during treatment. When using this option, the stereotactic coordinate system is defined by the

cone-beam image taken before treatment. A thermoplastic mask is used in combination with the IFMM system to account for the potential for increased patient motion when not using the frame. Since the opportunities for positioning misalignment and patient movement have been introduced to the treatment with these modifications, end-to-end testing was conducted to ensure that correction calculations for positioning and motion monitoring methods were being performed to sub-millimeter accuracy. Although end-to-end testing has been conducted acknowledging a motion tolerance of 1.5 mm motion during treatment [6], there has yet to be a detailed level of testing that incorporates a moving target to imitate common patient movements during treatment. These tests were not only conducted to ensure the same high precision and outstanding clinical results as the previous models but also to investigate the treatment accuracy at different levels of motion.

CHAPTER 2. BACKGROUND

In 1967, Dr. Lars Leksell of the Karolinska Institute in Stockholm, Sweden ordered the first gamma knife for construction. Although beginning as a prototype unit designed for functional neurological surgery, modern Gamma Knife radiosurgery has been used to treat over 300,000 patients and averages over 35,000 new treatment cases per year [13]. This method uses beams of highly focused gamma radiation from fixed Cobalt-60 sources that converge at a specified focal point to treat brain tumors, brain metastases, vascular malformations, trigeminal neuralgia, and other functional indications including Parkinson's disease.

The physics behind the GK system has remained unchanged with the use of the Cobalt sources. Cobalt-60 decays to stable Nickel-60 with the emission of one electron via beta decay and two gammas with energies of 1.17 and 1.33 MeV, which are used towards the clinical effectiveness of this device. The modern units of the Gamma Knife, the Perfexion and the Icon, incorporate an array of 192 sources with an inclusive collimation system that directs the individual beams of radiation to a superimposed focal point. At this point, a much higher dose rate is incurred, which is then used to target very specific areas of tissue without significant damage to surrounding normal areas in the brain.

As the goal with every stereotactic radiosurgery method, the Gamma Knife aims to deliver extremely precise high-dose radiation therapy in fewer treatments than conventional therapy. This provides the preservation of healthy brain tissue, as well as appeal to patients due to shorter overall treatment times. For most GK technology, a

restricted lesion size of 35 mm diameter or less is conventional, above which, effectiveness begins to decrease due to limitations on the utilization of radiation during delivery [13]. Traditionally, linear accelerators have been used to accurately treat every part of the body; however, the GK has long made clinical advancements in the treatment of the brain. So far, long-term results from this treatment have been documented as comparable to other, more commonly used methods of radiosurgery, such as stereotactic radiosurgery (SRS) delivered with linear accelerators. Additionally, when compared to conventional radiotherapy, the Gamma Knife delivers up to three times lower dose to normal brain tissue and up to one hundred times lower dose to the entire body [5].

CHAPTER 3. METHODS AND DESIGN

3.1 Overview

The testing that will be discussed in this thesis was done to verify the integrated imaging system by treating a shifted target to mimic patient misalignments, observing the system's ability to accurately correct patient shift during setup. Additionally, this work independently evaluated the motion tracking system by treating a moving target, mimicking patient movements underneath a mask during treatment, which observed the tolerance at which there was a clinical detriment to the quality of a simple treatment plan due to patient motion.

In the preliminary considerations for this work, it was understood that end-to-end testing for the Leksell Gamma Knife Icon system had been previously documented [6]. However, the results and conclusions from previous testing had not thoroughly considered the effects of patient movement on radiation delivery to the treatment target. With the modifications to the new GK system, which provides a frameless option for the treatment, there was an introduction of potential error due to allowed patient movement. As per a clinical study conducted at the Princess Margaret Cancer Centre in Canada [2], the tracking system upgrade in the Icon system provided an adequate way to track motion and deliver treatment to a seemingly stationary target. It was determined by the physicists at Emory Saint Joseph's that it would be beneficial to conduct testing of the system's ability to deliver radiation to a moving target instead, to ensure continued treatment accuracy as per the reputation of the stereotactic radiosurgery method. To carry out this testing, a phantom that could be used for stereotactic measurements was needed, as well

as a moveable platform device which could be rigidly attached to the chosen phantom and GK treatment couch, all of which are described in the sections that follow.

3.2 Leksell Gamma Knife Icon System

The Gamma Knife Icon system is separated into many parts, which are physically established into a control room and a treatment room. The control area includes the operator console and the Leksell GammaPlan treatment planning software, and the treatment room houses the Icon unit, which includes the patient positioning system, CBCT gantry, and the IFMM system. Since this work focuses on the verification and evaluation of the CBCT and IFMM respectively, the following sections will give concise details on each system.

3.2.1 Cone Beam Computed Tomography

The C-arm is attached to the most superior location on the gantry of the Icon unit. It is generally used for two types of scans, which include the stand alone-scan that defines the stereotactic coordinate system for the frameless treatment option and the treatment scan, used to verify the patient's position at the time of treatment. The C-arm is attached to the tilt arm, as seen to the left of the unit in Figure 1, which makes it possible to move from the parked position to the position that conducts the CBCT scan. It is a rotating unit that travels from this scan position through a 180 degree half-scanning path around the patient to capture the image and houses an attached X-ray tube and image detector for acquisition efficiency [6].

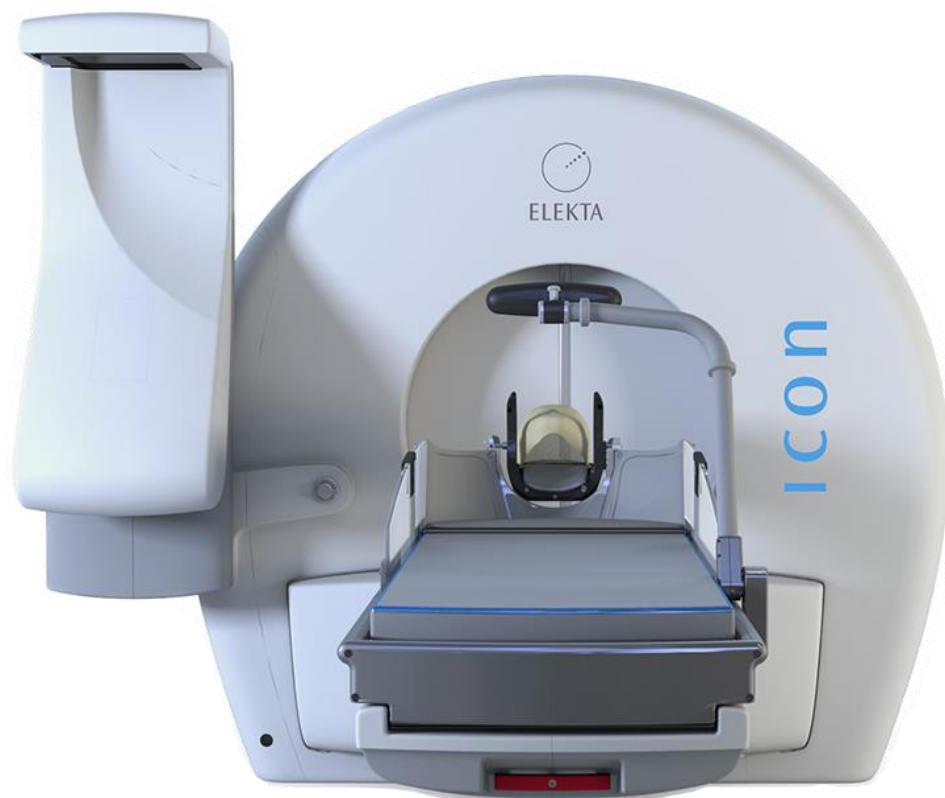


Figure 1 - Front view of the Leksell Gamma Knife Icon system with C-arm attachment upright in the parked position [5]

For each test conducted in this work, the C-arm was used to ensure that any offsets of the target location, mimicking a patient's daily difference in setup position, was properly accounted for in the treatment planning system and the resulting shifts to the patient's position align the shots of radiation to the same anatomical position as the location in the stereotactic setup and established plan. Since end-to-end testing will be conducted using different levels of motion, the C-arm was used to both define the stereotactic coordinate system for each level and position the Lucy phantom for treatment each time the level of allowed motion is altered.

3.2.2 Infrared Motion Management (IFMM) System

As previously mentioned, the difference between the Icon system and its predecessors is its ability to provide a frameless, noninvasive gamma knife option. This option introduces potential error to the stereotactic method by gifting the patient with the ability to move during treatment underneath the thermoplastic mask that is used in lieu of a titanium alloy frame. Since the immobilization capability of the frame remains unparalleled, preliminary evaluations of the thermoplastic mask immobilization system performed by Winnie Li et al. [11] demonstrated and confirmed the need for both on-board CBCT and infrared (IR) tracking to achieve intra-fraction motion management of the target during treatment. Thus, the infrared motion management system, also referred to as the high definition motion management (HDMM) system, is used to monitor patient movements during setup and throughout the treatment as the second component to the modified GK system to permit the use of the frameless treatment option.

The IFMM system, as shown in Figure 2, consists of an infrared stereoscopic camera, a reflective patient marker, and the reference markers in the mask adapter, which connects to the patient's mask and attaches to at the GK unit. The silver, circular reference marker is applied to the nose of the patient during setup on treatment day, as shown in Figure 3. The infrared camera is mounted onto an extension on the couch and tracks the patient at a frequency of 20 Hz with an accuracy of 0.1mm using the patient and reference markers [4].

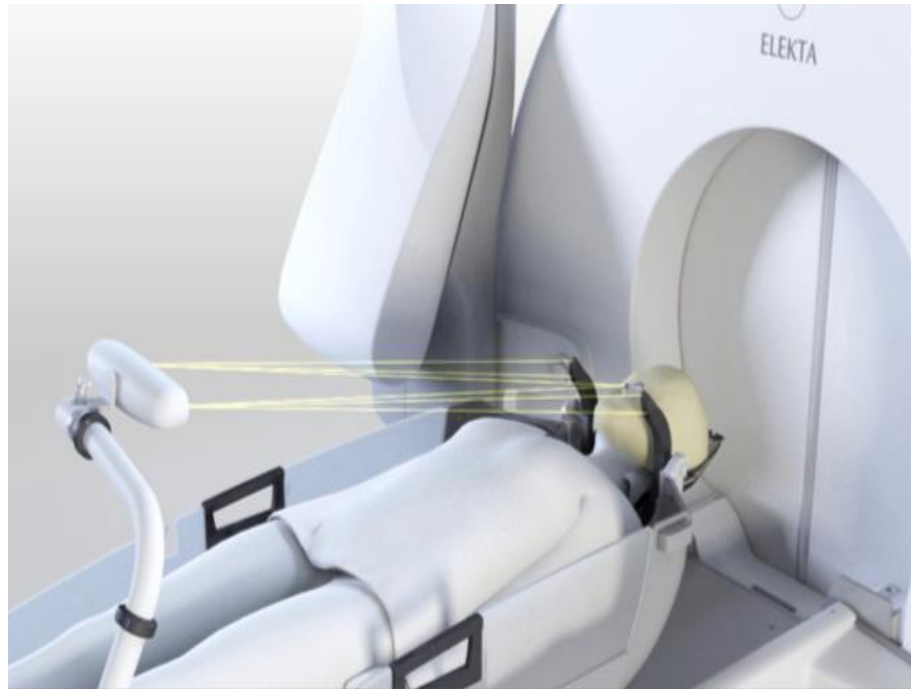


Figure 2 - The infrared motion management (IFMM) system with highlighted tracking paths from the infrared camera to the reference markers on the nose of the patient and in the mask adapter [4]



Figure 3- Patient in the mask adapter with nose marker and thermoplastic mask [4]

When the IFMM is recording patient movement, a graph is shown in the graphic user interface (GUI) in both the treatment room and in the control area, where the motion is recorded in mm from the starting position and the time duration is in seconds. According to Elekta, the default movement tolerance for a patient during treatment is 1.5 mm, which is considered an active setting because it limits the amount of motion allowed during treatment. However, the tolerance can be passively set up to 3.0 mm, in which the system does not pause if the patient moves above this limit [6]. Passive treatment is not typically used in clinical settings. During treatment under the active tolerance setting, if the patient moves out of tolerance for more than two seconds, the treatment is paused, and the operator is alerted. As a safety feature, if the patient stays out of tolerance for more than 30 seconds, the machine interrupts the treatment moving the patient out the unit and blocking the sources from administering radiation. If the patient does not move back into tolerance, another treatment CBCT must be taken to account for shifts in the setup of the patient before the treatment can be continued.

It is important to keep in mind that although the motion tolerance level is set with respect to the movement at the marker on the nose, the movement of the intracranial tumor or other target areas in the brain is the real concern. For this work, the IFMM was evaluated for different levels of possible patient motion, ranging from around 0.5 mm motion at the nose of the phantom to the extreme case of 5 mm. As mentioned, the purpose behind this range is to observe the clinical detriment at which the system and corresponding treatment plan begins to fail for accuracy. The platform has both horizontal and vertical motion capabilities and will therefore be used to evaluate the IFMM for patient motion in the corresponding planes.

3.3 Patient Workflow for Frameless Treatment

Since this work was done to conduct end-to-end testing of the Leksell Gamma Knife Icon system, the procedure was written to imitate normal patient workflow. Therefore, for comparison, it is beneficial to provide the treatment workflow for a patient being treated on the GK with thermoplastic mask fixation and stereotactic references defined by the on-board cone-beam CT imager as given in [6].

On the first day of the patient's treatment process, a non-stereotactic simulation image is taken using a magnetic resonance (MR) imager or CT to provide anatomical information for treatment planning. MR is the preferred method due to its popularity with the soft tissue imaging of the brain; however, if the patient is dependent on special devices, such as pacemakers, CT will be used due to its lack of magnetism. During this simulation, both the thermoplastic mask and a custom pillow needed for setup are fit to each patient for treatment immobilization and reproducibility. The patient is then taken to the treatment room, where the pillow and cushion is molded onto the mask adapter and a stand-alone CBCT on the Icon system is obtained to get the stereotactic reference coordinates for the treatment planning. The simulation image is then imported and co-registered to the reference CBCT image using the Leksell GammaPlan for treatment planning, review, and approval.

On the following treatment day, the patient is setup on the treatment couch in approximately the same location as the simulation day using the fixation mask and molded pillow. When the patient is in position and the treatment is loaded, the IFMM is activated to begin tracking patient motion. A treatment CBCT is taken to correct for

shifts that cause the patient target anatomy to deviate from the location coordinates of the target during the reference setup, from which the treatment plan was created. Once all parameters are corrected and approved, the treatment is administered as pre-planned by the administering physicist. Each time the patient moves and stays out of tolerance and for each treatment fraction, the setup, imaging, and treatment delivery workflow is repeated.

3.4 Lucy 3D QA Phantom

As mentioned, a phantom that could be used for stereotactic measurements needed to be either chosen or manufactured for this project. The Lucy Three-Dimensional (3D) Quality Assurance (QA) Phantom, or Lucy, was designed by Standard Imaging, Inc. for quality assurance testing of entire stereotactic radiosurgery procedures and was chosen for this project for its availability and feasibility of our predetermined testing needs. The phantom is shown in Figure 4 mounted to the precision leveling and rotational alignment base, which was not used in this work. Lucy is compatible with angiographic, MR, and CT imaging modalities making it a great tool for stereotactic system end-to-end testing and process verification. The spherical, radiopaque phantom is manufactured out of Lucite plastic, from which the name is coined, and has a diameter of 140 mm. It is separated into upper and lower hemispheres and is held together by embedded plastic screws (Figure 5), with middle cavities included for holding accessories determined by the test at-hand. These accessories include but are not limited to ion chamber inserts, film cassettes, marker cylinders, volume and grid inserts for CT scans, and volume inserts and signal generators for magnetic resonance (MR) scans.



Figure 4 Lucy 3D QA phantom mounted onto the precision leveling and rotational alignment base [17]

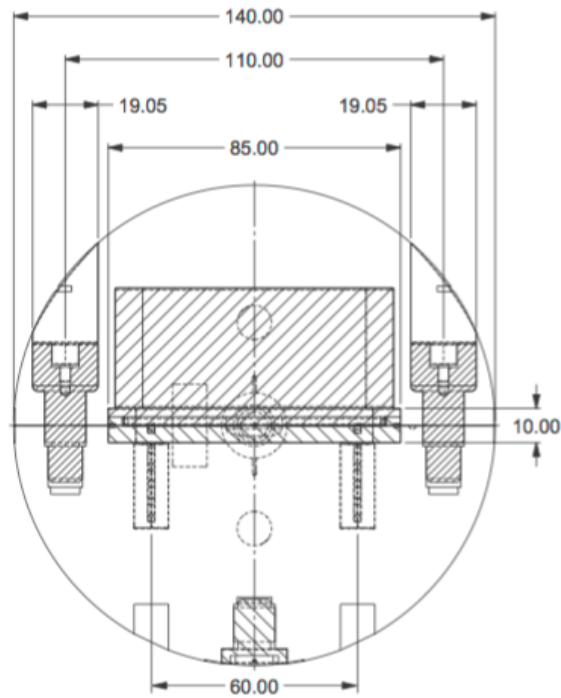


Figure 5 Lucy 3D QA phantom design with spherical dimensions in mm [17]

3.5 Phantom-Platform Device

3.5.1 Platform Design

The platform device was designed specifically for this work and was manufactured by Matthew Carroll of the Georgia Tech machine shop. Figure 6 shows a drawing of the device from the overhead view with labeled parts and dimensions in inches. It is approximately 23.75 inches long and 8.887 inches wide and was designed to rigidly attach to the mask adapter, used during gamma knife treatments to hold the head of a patient, while resting the motor and electronics in an enclosure on the treatment couch. The rigid attachment incorporates a semi-circular offset neck and plastic screw that was designed to attach the Lucy phantom in an orientation mimicking the head of a patient during treatment. The offset became a hindrance to the level of allowed motion along the vertical axis, which will be discussed later in this section.

The pivoting frame was made from nylon polyamide plastic, which was chosen as not to severely contribute to the attenuation of the gamma rays during the delivery of the plan. There is a screw hole on each of the four sides of the pivoting frame, designed to determine the direction of allowed motion once the device is powered on. For instance, if the top and bottom plastic screws were in place, only the horizontal motion was allowed. Conversely, if the side screws were implemented, a vertical motion was allowed, which was included to imitate the most common patient movement at the chin of the thermoplastic mask.

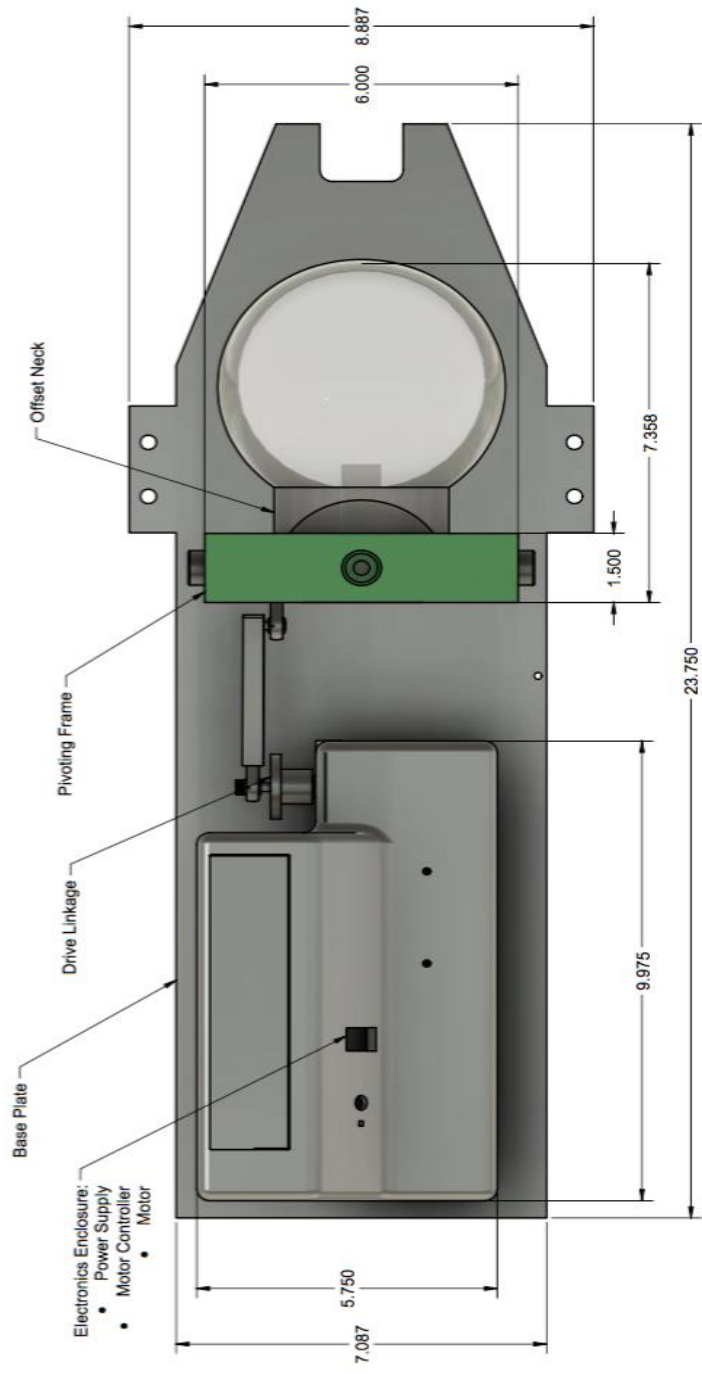


Figure 6 - Drawing of the phantom platform device (overhead view) with dimensions given in inches

The back half of the platform, which rested on the treatment couch, is connected to the previously described forward design of the device by way of the base plate and driving linkage. The drive linkage screw positions and the attached crank on the posterior end of the linkage are what determined the allowed range of motion in the vertical and horizontal directions. There were a total of four interchangeable metal cranks that varied only in the placement of the center offset hole position. These cranks included 0.025, 0.050, .0.075, and 0.100-inch offsets labeled on the surface of each, as shown in Figure 7.

The difference in offset position from the center of the crank allowed for different levels of phantom motion when the device was powered on. For the vertical direction, only the 0.025-inch offset crank was used due to physical limitations of the platform. When other cranks were tested while the platform was in the orientation to produce vertical motion, they resulted in levels of motion that caused the posterior end of the plastic screw that attached Lucy to the pivoting frame to collide with the top of the frame due to the offset placement of the connecting hole. This would cause unwanted jumps during the motion and consequently in the motion-tracking graph on the GUI, which made measurements with cranks larger than 0.025-inch more troublesome. Instead, one crank was used, and the length of driving linkage was adjusted to produce different levels of motion in the vertical direction. For the horizontal direction, on the other hand, each of the offset cranks was used to allow different levels of motion. The motions were then fine-tuned for comparability to the vertical direction by adjusting the position of the driving linkage. These changes in the levels of motion were imperative for the evaluation of the infrared motion management system and its ability to monitor movement during treatment. The testing workflow, which includes the levels of achieved motion from the

change in driving linkage position and offset crank, will be further discussed in Section 3.7.



Figure 7 - Offset cranks that determined the levels of motion for the device

Lastly, the back portion of the platform contained the electronics enclosure, which was 3D printed with blue styrene plastic. The enclosure housed a 12V DC motor, a DMC60 digital motor speed controller, an Arduino Leonardo microcontroller to read the position of the knobs that controlled the speed, and a 12V power supply. The turn switch that controlled the speed of the device was located on top of the enclosure, and the device had two power switches, one next to the turn switch and one on the back end of the enclosure underneath the power cord.

3.5.2 Platform Motion Geometry

Although designed to imitate normal patient movement, the levels of motion produced by the platform in this work were of extreme consideration. This was due to the fixed location of the film inside of the Lucy phantom film insert in relation to the nose that was placed on surface of the phantom. The film was located approximately 100 mm from the center of the pivoting frame, whereas, the nose was placed closer, at approximately 60 mm from the frame. Since the C1 vertebra in the neck is the most natural pivoting point for a human head, it is possible for this geometry to occur when considering a real patient. This would be a case in which the vertebra is closest to the nose and furthest away from the tumor. However, it should be noted when considering the data acquired from this work that this was a very specific geometric case, in which the “tumor” location was much further from the pivoting point than the marker location at the nose in the horizontal plane. This would impact the movement at the film in relation to the movement at the marker on the nose by magnifying the target motion at the center of the phantom in all planes considered for this work.

Figure 8 is an illustration of the effects from the setup geometry on the level of motion allowed at both the film in the middle of the phantom and the nose marker at the surface of the phantom. This will be further considered for the effects on the acquired data in the results section of this report.

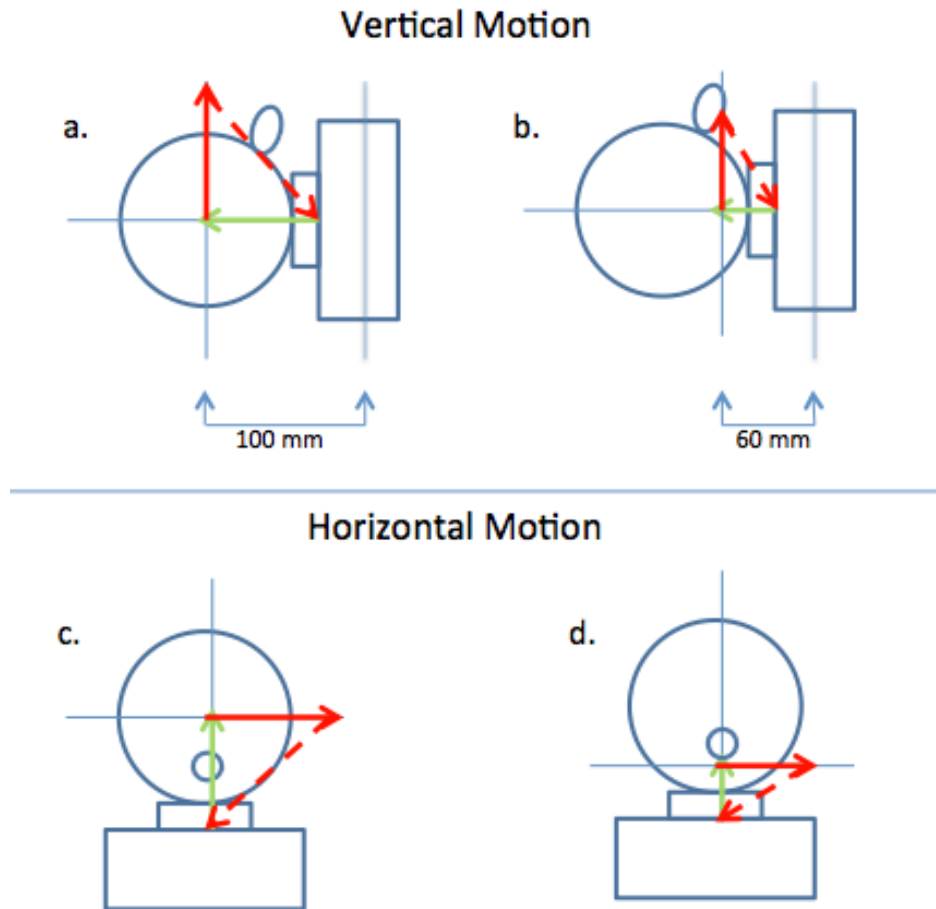


Figure 8 - Effects of the platform-phantom geometry on the level of motion allowed at the centered film and at the nose of the phantom. Diagrams a. and b. are side views of the levels of motion allowed in the vertical plane at the film and nose, respectively, due to their locations along the pivoting axis (in green). Diagrams c. and d. are overhead views of allowed motion in the horizontal plane at the film and nose, respectively.

3.6 GAFChromic EBT3 Dosimetry Film

For this project, the treatment plan was delivered to the Lucy 3D QA Phantom containing GAFChromic EBT3 film from lot number 05011701. GAFChromic EBT3 dosimetry film was developed to address the needs of dosimetrists and medical physicists in clinical environments by measuring absorbed doses of ionizing radiation, particularly high-energy photons. It is suitable for testing applications such as those conducted using image-modulated radiation therapy (IMRT), volumetric arc therapy (VMAT), and brachytherapy, exhibiting its highest performance in the dose range from 0.2 to 10 Gy. The structure of the GAFChromic EBT3 film is comprised of two outer layers of matte-polyester substrate each with 125 μ m thickness and a 28 μ m-thick inner active layer containing marker dye and stabilizers, which yields a nearly energy-independent response of the film. The active layer is so called because when it is exposed to ionizing radiation, it reacts when the absorption maxima is at 633 nm to form a blue polymer, which shows through the clear outer layers of the film. Figure 9 shows a drawing of the film structure as described.

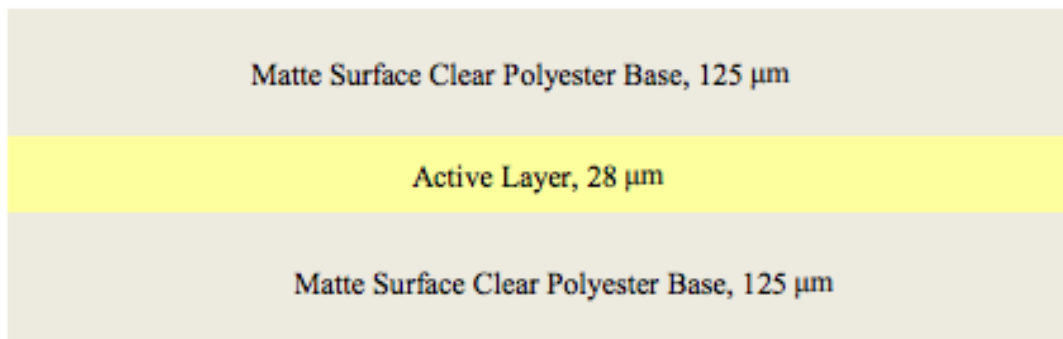


Figure 9 Structure of GAFChromic EBT3 Dosimetry Film [9]

Like its predecessors, EBT3 film is self-developing through a polymerization process, which is an induced chemical reaction of the monomers in the active layer of the film. To fully utilize this feature, the film must be exposed and digitally scanned 24 hours after irradiation, which is the peak of its self-development. The film has minimal energy dependence from 100 keV into the MV range, making it safe to handle in interior room light for short periods of time without altering the darkening of the film. However, as per [9], it is advised for the film to be stored in the dark away from radiation sources at temperatures below 25 degrees Celsius as a precaution.

3.7 Leksell GammaPlan

The Leksell GammaPlan is a treatment planning system designed specifically for Leksell Gamma Knife stereotactic radiosurgery models. Planning is based on processing projectional and tomographic images using a computer workstation running the software. GammaPlan can handle acquired images from modalities such as computed tomography, magnetic resonance imaging, positron emission tomography (PET) scanners, and angiograms (AI), all of which allow direct comparison of vascular and tissue structures. The workflow of creating a plan in the GammaPlan system includes defining the targets and treatment dose, configuring the treatment collimators, and determining the shots of radiation to be delivered by the Icon system [7].

Due to minimal moving parts in the Leksell Gamma Knife models, GammaPlan is known and revered for its simplicity. Since the models have inherent accuracy, safety, and reproducibility features, the main area that GammaPlan is designed to perfect is the

precision science for delivering very high intensity shots of radiation to the correct intracranial locations. The software does not have any remote control during the radiosurgery procedures; therefore, a plan including the correct structure definition and shot placement must be established, reviewed, and approved for final use before the treatment begins.

The sub-millimeter accuracy of the GK models is obtained with the incorporation of the stereotactic coordinate and reference system that is shared with the Leksell GammaPlan for each patient during treatment planning. Two ways to define the stereotactic reference coordinates are by using the indicator box for the Leksell Frame G during image acquisition and with the use of the on-board CBCT imager only available on the Leksell Gamma Knife Icon System. This work is focused on the frameless treatment option for the Icon, and therefore, only the reference system as defined by the CBCT will be discussed. Since the CBCT is an integrated part of the newer Icon system, the entire system is calibrated for the same spatial reference. The CBCT spatial reference was made to match that of the machine, so no other external reference, such as the indicator box with the frame, is needed.

3.8 End-to-End Testing Procedure

3.8.1 Platform Setup

First, the decision was made that the “nose” of the Lucy phantom would be a hollow, plastic ion chamber holder that was filled with tissue equivalent aquaplast

thermoplastic pellets to reduce air gaps and beam scatter. It was then wrapped with tape to eliminate reflective interference to the IFMM from the plastic surface. The surface of the phantom was also taped and wrapped in Bandnet tubular elastic dressing to further minimize reflective surfaces. The nose was attached to the surface of the phantom using double-sided adhesive tape, and an infrared reflective sticker was placed on its surface to be seen by the IFMM. The complete setup from this work with the QA phantom is shown in Figure 10.

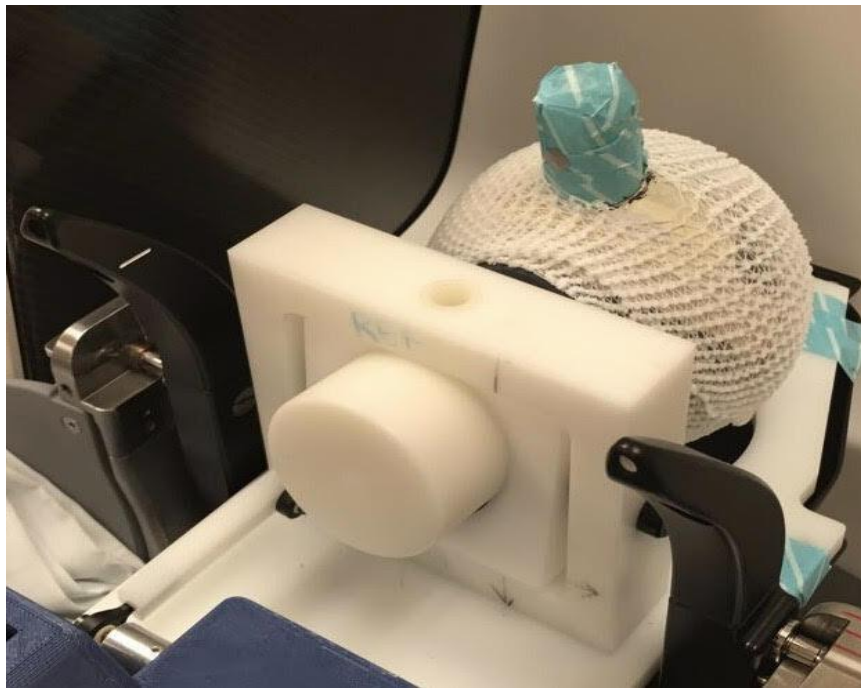


Figure 10 The Lucy phantom attached to the platform device in the mask adapter, with nose marker and non-reflective surface coverings

The Lucy phantom housing the film cassette insert with fiducial markers, was connected to the platform device and a simulation CT image was obtained using a Philips CT Big Bore scanner. This scanner is used daily at Saint Joseph's and provides a 60-cm true scanning field of view for a multi-sized patient population, as well as spatial

positioning accuracy of less than 2 mm, as required in the American Association of Physicists in Medicine (AAPM) Task Group 66 (TG-66) protocol [15]. The simulation image was then reconstructed and sent to the Leksell GammaPlan for planning. MRI was not used for this work, as it would be in normal patient workflow, due to the lack of image contrast that would result from imaging the radiopaque phantom. The fiducial markers in the phantom would not be visible in MR, rendering the image of no use for this project. Additionally, regarding the simulation in normal workflow, a thermoplastic mask and pillow were not needed.

For this work, only the film cassette insert was used to hold film in the center of the Lucy phantom during dose delivery to emulate a centered intracranial tumor. GAFChromic EBT3 film was cut into approximately 5x5 cm squares that fit inside of the film cassette insert of the Lucy phantom, as shown in Figure 11, to be irradiated during these tests. The insert had a pinprick in each of the corners of the square plug-in, with two pricks in what was considered the upper right corner. Since GAFChromic film orientation is extremely important for absorbed dose measurements [8], the corner of the plug-in with two pricks was beneficial in keeping both the alignment and orientation accurate. After the film squares were irradiated, they were labeled with the film number, which sorted them by the level of motion used for each delivery. Section 3.9 offers further details of the GAFChromic film and the film calibration process.



Figure 11 - Overhead view of the film cassette insert inside of the Lucy phantom

The phantom-platform device was taken to the treatment room and attached to the treatment couch using the mask adapter, which was then secured with blue clinical tape. To hold the platform at a firm flattened position, solid water blocks were used in the space between the mattress of the treatment couch and the posterior end of the device. Figure 12 is an overhead view of the setup that was maintained throughout the duration of this work. In this position with the motion powered off, a stand-alone CBCT was obtained at the beginning of the workflow for each level of motion, which defined the stereotactic coordinate system.

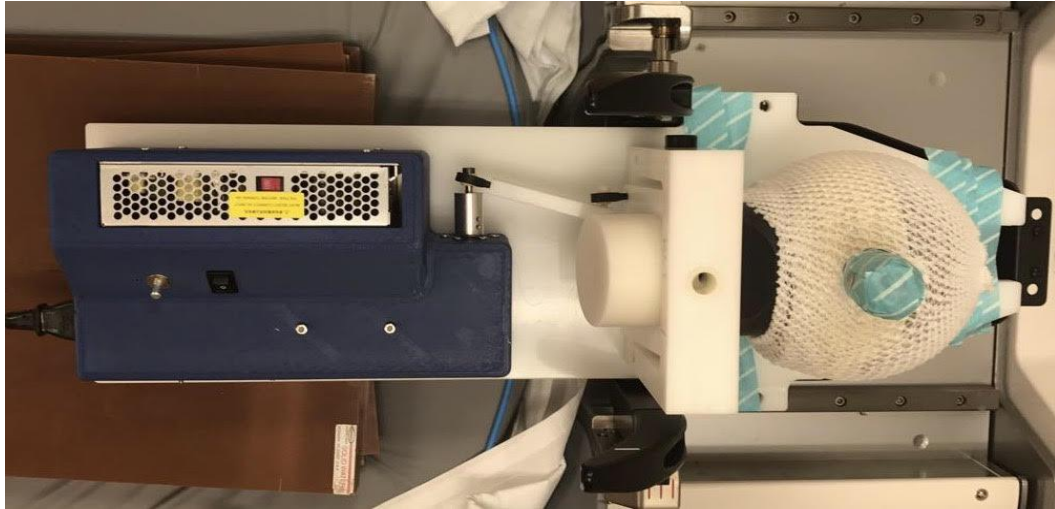


Figure 12 - Overhead view of the phantom-platform device holding Lucy in an orientation mimicking the head of a patient during treatment

3.8.2 Simplification of the Treatment Plan

With popular treatment equipment, such as linear accelerators, operators have the option to input a certain number of monitor units, calibrated to the amount of dose delivered to the target, which can then be quickly delivered once all interlocks on the device are clear. However, in gamma knife systems, there is a specific workflow that must be followed before each irradiation. This begins with the planning of a treatment designating parameters such as the coordinates for the location of the target, the amount of radiation to be delivered, the radiation prescription isodose line to the target, and radiation collimation. In the control area, treatment planning using Leksell GammaPlan began as it would in normal patient workflow, with a target shot being placed at the center of the film holder using the fiducials in the simulation CT. Then the simulation CT was co-registered to the reference CBCT to locate the target area coordinates for which the radiation shot would be placed. A simplification for this work was that treatment plans of only one 16 mm symmetric radiation shot was delivered. This could be

considered a worst-case scenario for actual patient treatment because it results in a sharper gradient, where there would be more dramatic dose differences at the edges than in a more complex plan with shallow dose fall-off. Nevertheless, single shots are sometimes clinically used for mask patients, and therefore, a simple treatment plan of just one 16 mm target shot was determined to sufficiently evaluate the capabilities of the integrated imaging and motion management systems for the Leksell Gamma Knife Icon.

3.8.3 CBCT and IFMM Evaluation

The shot was planned to deliver 5 Gray (Gy) to the 100% line of the target, which is at the center of the target area, determined to be 100.3, 138.4, and 79.5 in Cartesian coordinates. This was numerically based off the reference CBCT coordinates but visually based off the CT simulation. The co-registration of the treatment CBCT and the reference CBCT began the evaluation of the integrated CBCT imager, which would be monitored for accurate shot placement through the entirety of the project for each change in motion level. Due to a limitation of the design having no home or base position, the stereotactic coordinates were different at each level of motion to account for the shifts acquired from removing the phantom to insert new film between each test. The goal was that each resulting shift determined by the cone-beam taken at each level, would place the shot in the same anatomical position as the initial shot position.

As a baseline for later treatment comparison in the data analysis, the first plan was delivered to the Lucy phantom in a stationary position, meaning there was no motion from the platform. The plan was conducted in 1.9 minutes, or 114 seconds, delivering 5 Gy to the center of the target film. Next, the task was to deliver the same plan to a

moving target, in which the Lucy phantom would consistently oscillate along one axis (either vertical or horizontal) at varying levels of motion. The levels of motion were determined by the manipulation of the screws connected to the driving linkage and the interchangeable cranks, as described in Section 3.5. Once the film was changed and the platform was put back together after each adjustment, the motion was turned on and observed for approximately two minutes on the GUI in the treatment room to allow the motion to become as consistent as possible. After a consistent range was determined, the platform was stopped at a documented midpoint in the range of motion, in which the position was held for acquisition of the CBCT. The C-arm was manually driven to the scanning position before leaving the treatment room in preparation for the treatment CBCT (CBCT_t) that would make the necessary shifts to place the shot in same position in the phantom as in the original plan. The CBCT_t acted as a zeroing factor for that specific position, meaning that once the motion began again, there would not be any oscillations below the current position, shown as zero on the GUI. Instead, the graph would show a continuous oscillation above the zeroed position that would only track how far away the infrared marker on the nose would get from the chosen (baseline) position. This yielded the experimental value of the level of motion at the nose of the phantom that will be compared to the measured level of motion in the center of the film. This is important since in normal patient treatment, the marker and monitoring of the movement nose is simply a surrogate for the movement of the tumor, which is the real concern.

Once satisfied with the obtained level of motion, the plan was delivered to the phantom while the platform continued oscillating along the chosen axis. After the plan was delivered, a CBCT was taken at the maximum point in the range of motion (CBCT_m)

to measure the total displacement from the baseline of the range. The $CBCT_m$ and the $CBCT_t$ were both used to determine the measured amount of motion at the center of the film by taking the difference in Cartesian coordinates of the fiducial markers shown on the images in reference to the Leksell coordinate system. In the data analysis, this value for the motion at the center of the film, which is the primary concern in clinical settings, was compared to the movement at the nose.

After each irradiation, the Lucy phantom was taken apart, the irradiated film was marked, and a new piece of EBT3 film was inserted in the proper orientation as shown in Figure 11. The importance of film orientation for film calibration and analysis will be discussed in the following section. After the new film was inserted and Lucy was reinstated on the platform, the above steps for the moving platform treatment delivery were carefully repeated for each obtainable level of motion. Since two CBCT images were taken per film, the dose from these images was also considered in the data analysis of each irradiated film.

3.9 Absolute Film Dose Calibration

3.9.1 Optical Density

When discussing dosimetric film, the most important parameter is radiographic density, or optical density (OD), which is a measure of the degree of film darkening after exposure. It is defined as the logarithm of the ratio of the incident intensity (I_0) on the

film to the intensity of transmitted light (I_t) through the film. This is written mathematically as

$$OD = \log\left(\frac{I_0}{I_t}\right) \quad (1)$$

Generally, the absorbed dose to the film is proportional to the change in optical density, where the change in optical density is defined as the exposed optical density minus the unexposed optical density. To consider changes to the film due to background radiation, a piece of film used as a control is monitored, and the change in the control OD is subtracted from the change in OD from the exposed film, shown as

$$\Delta OD_{net} = OD_{exposed} - OD_{unexposed} - (OD_{control,after} - OD_{control,before}) \quad (2)$$

where $OD_{exposed}$ and $OD_{unexposed}$ are the optical densities of the exposed and unexposed film, respectively, and $OD_{control,after}$ and $OD_{control,before}$ are the optical densities of the control film before and after exposure to account for background radiation.

Therefore, by substituting equation (1) into equation (2), an expression for the net optical density in terms of intensity is obtained as

$$\Delta OD_{net} = \log\left(\frac{I_{unexposed}}{I_{exposed}}\right) - \log\left(\frac{I_{control,before}}{I_{control,after}}\right) \quad (3)$$

where $I_{unexposed}$ and $I_{exposed}$ are the intensities of the test film before and after its exposure, respectively, and $I_{control,before}$ and $I_{control,after}$ are the intensities of the control film before and after the time of exposure, respectively [10].

3.9.2 Film Calibration

Ideally, a product of any type would produce test results that matched with no error to every point of the sampled values within the calibrated range. However, this is not true for anything, especially not dosimetric film used for clinical measurements, where the environment is constantly changing due to several factors. This includes factors such as the usage of a piece of equipment, variations in equipment calibration, and time differences in regard to the amount of film darkening allowed during self-development. For analyzing film used for dosimetric measurements, absolute dose calibration is important because film darkening is not a linear occurrence; rather it is seen to be an exponential or piecewise function.

With all versions of GAFChromic film, it should be noted that consistency in the orientation of the film when it is cut and consequently when it is scanned for digital calibration is imperative. In the preceding film models, EBT1 and EBT2, both orientation and film side placement were important due to the different thicknesses of the outer polymers, which protect the active layer of the film. However, the EBT3 provides equal outer thicknesses making only consistency in orientation important due to symmetry. Once film calibration is conducted, inconsistent orientation of the film has been observed to cause up to a ten percent discrepancy in the dose and dose distribution, which leads to faulty data analysis. Film handling should be done with extreme caution, preferably by the edges of the film using gloves. Fingerprints or debris on the film surface may be problematic during scanning and digital analysis. For this work, the EBT3 film was cut with a guillotine cutter in approximately 5x5cm squares and marked in the upper right corner to keep the vertical orientation consistent in relation to the original sheet. The

vertical orientation was held constant for both the calibration exposures and for test measurements as per the protocol [8].

After the film was cut for calibration, treatment plans were made using Leksell GammaPlan to deliver one shot of radiation to the center of a piece of film in consecutive doses of 1, 2, 3, 4, 4.5, 5, 5.5, 6, 7, and 8 Gy. The film calibration sphere, which is a GK dosimetry tool, was attached to the head of the treatment couch and used to hold the films in the head of the machine during irradiation. After each exposure, the film squares were labeled with the administered dose and a new square was inserted for the next delivery. A piece of the film was also set aside as a control with no dose being delivered. Recall Equation 2 in the previous section. In normal calibration calculations, the dose from the control piece at the scanning time 24 hours later would be subtracted from the other irradiated squares to account for possible background radiation dose to the film. However, the Radiation Imaging Technology (RIT113) dosimetry software, which was used for this calibration as well as the dose measurements for the project, was not programmed to consider background radiation dose significant due to improvements in the uniformity of the film. Therefore, the 0 Gy film was only used as a starting point for the data collected to generate the calibration curve, as opposed to a correction factor for the change in optical density of the film.

When discussing film calibration, it is additionally important to consider how the Leksell GammaPlan treatment planning system calibrates dose to be administered to the films. Due to the complicated partial-hemisphere arrangement of the Cobalt-60 sources and the rigid geometry of the Gamma Knife, there is currently no officially accepted protocol for the dosimetry of the device [14]. However, a modified version of the

American Association of Physicists in Medicine (AAPM) Task Group 21 (TG-21) protocol using air kerma based dosimetry, a solid water phantom, and an air ionization chamber is widely used [12]. AAPM Task Group 51 (TG-51), an updated version of TG-21, calls for the utilization of Farmer chambers in water phantoms for clinical reference dosimetry measurements [1]. It requires absorbed dose to water calibration factors, making the measurements, concept, and implementation of this method easier than earlier protocols. The absorbed dose-to-water factors are needed because the thin electrode, or collector, in a Farmer chamber is surrounded by graphite, which acts as an insulator to generate the electric field needed to measure the dose and is also water and tissue equivalent [3]. Although the Leksell GammaPlan is calibrated using these absorbed dose-to-water factors, the dosimetry Task Groups, were written for teletherapy beams only, in which the radiation originates at a single source that is broadened to form a uniform field. This is a very different consideration from the 192 radiation sources of GK, which focus at a single point in the head of the machine. Conclusive testing of TG-21 with corrected air kerma dosimetry [14] has been conducted and deemed acceptable for the calibration of the GK until a formally accepted method is implemented. Therefore, the dose that is calibrated with absorbed dose factors by the Leksell GammaPlan to be delivered by the Icon, which itself is widely calibrated with air kerma dosimetry, yields a delivered dose that is slightly lower than the expected value. The tolerance for this discrepancy has been evaluated, accepted, and established until future protocol acceptance is obtained.

3.9.3 Absolute Dose Calibration Curve

As mentioned, the GAFChromic EBT3 film must be digitally scanned 24 hours after irradiation to give the film time to self-develop as well as to prevent any extra darkening from exposure to background radiation, such as light. The Epson 11000XL scanner, which is the recommended scanner model for GAFChromic film [9], was used to digitize all film in this project. The scanner utilizes 48-bit color, which activates three-color channels (Red-Green-Blue) with 16-bits per channel, and 400 dots per inch (dpi) resolution, which corresponds to 0.1 mm per pixel. During the film import however, only the Red color channel was used for display, corresponding to the greatest change in optical density in GAFChromic film. The Epson 11000XL scanner response to exposed GAFChromic film is given by

$$X(D,n)=a+b(D-c) \quad (4)$$

where D is the dose administered and a , b , and c are constants. This behavior of GAFChromic film is rationalized by the fact that the film becomes less transparent as the delivered dose increases and the response asymptotes at very high doses [8].

Both the film calibration and analysis were conducted using the classic version RIT113 V6.3 of the RIT software. As previously discussed, this software does not take into consideration dose from control film that would take into account the change in the optical density of the film from background radiation as considered in Equation 2. Instead, only the irradiated film from each delivered dose is analyzed with the assumption

that each piece of film had no dose before the irradiation and was also unaffected by a background dose during the 24-hour self-development before they were scanned.

To generate the absolute dose calibration curve, the RIT software calculates the full-width half maximum (FWHM) of the dose distribution by the optical density of the scanned film. Each film square is analyzed separately so that the center of the FWHM is chosen to be the point at which the full amount of dose from the delivery was prescribed. A pixel value corresponding to the prescribed dose is given to that point and plotted. Figure 13 shows the absolute calibration curve generated by this method for the GAFChromic EBT3 film used in this work. During data analysis, this calibration was applied to each film before analysis was conducted in the software to correct for the exponential nature of film darkening and the variability in exposure conditions.

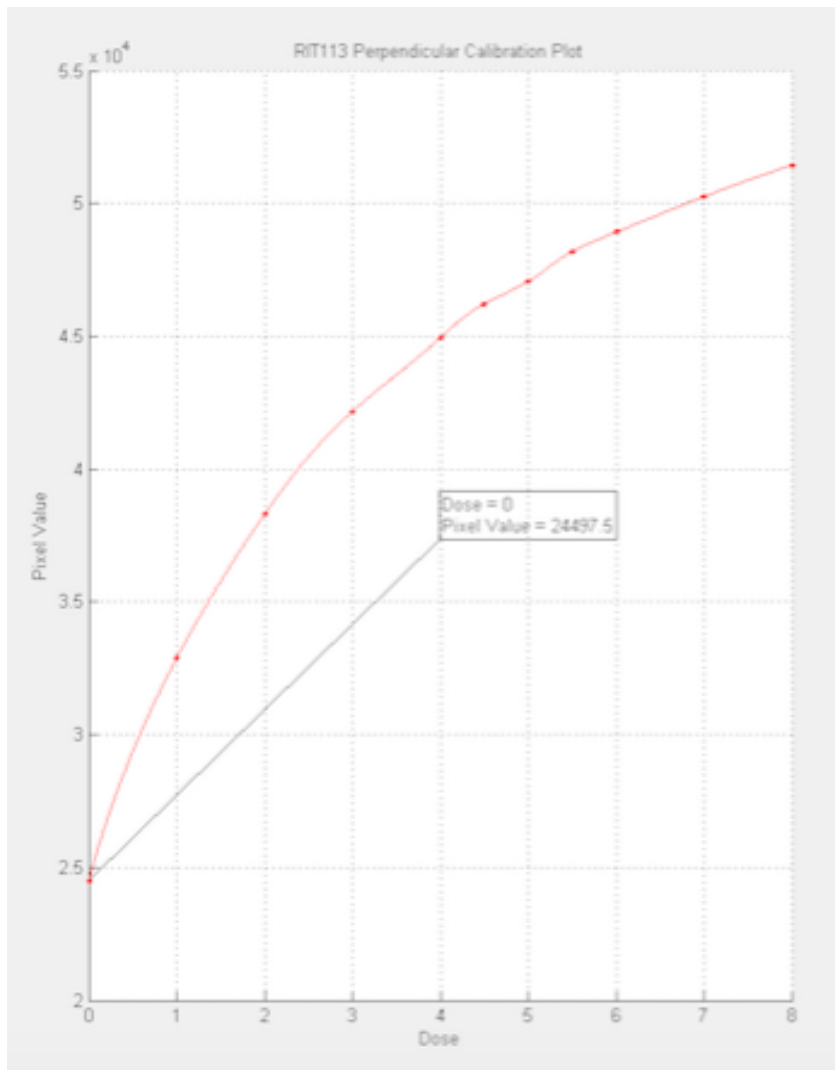


Figure 13 - The absolute calibration curve for the GAFChromic EBT3 film from lot number 05011701, where the Dose is given in Gy

CHAPTER 4. RESULTS AND DISCUSSION

4.1. Experimental vs. Measured Levels of Motion

As described in Section 3.2, the infrared camera that tracks the movement of the patient during frameless treatment on the GK does so by monitoring the displacement of the marker placed on the nose of the patient relative to the reference markers in the mask adapter (Figure 2). However, recall that the nose movement is solely a surrogate for the motion of the tumor during treatment, which is the real concern. Elekta, the manufacturing company of the Leksell Gamma Knife, stated in [4] that the movements observed by the HDMM at the nose are larger or equal to actual target movements in the skull of a patient. Therefore, although the default tolerance of movement at the nose is set to be 1.5 mm, this should only correspond to sub-millimeter movements at the tumor. Observations from this work dispute the universal proclamation from Elekta that movement at an intracranial tumor is less than what is seen at the nose.

Table 1 and Table 2 show the levels of motion and corresponding crank used to produce that motion in the vertical and horizontal planes, respectively. Recall that in the vertical direction, only the 0.025 mm crank was used and the screws on the driving linkage were adjusted to produce motion level variation. As described in Section 3.8.3, the experimental value was obtained at the nose of the phantom using the level of motion as seen by the IFMM, and the measured values were calculated using vector analysis of the displacements yielded from the CBCTs taken at the baseline and maximum point in each range of motion.

Section 3.5.2 gave an account for the geometry of the phantom-platform setup, which was a key factor in the differences of allowed movement at both locations during these tests. For the geometry used in this work, a trend was noticed that the movement at

the film was greater than the movement at the nose, experimentally observed with the IFMM system in all films except for Film 4. As previously mentioned, challenges were faced in the vertical direction to produce different levels of motion using one crank due to the physical limitations of the platform. Considering these limitations, how the phantom moved and drifted due to collisions with the pivoting frame and increased amounts of motion was a cause of experimental uncertainty. Since the measured motion in the table was calculated from the CBCTs taken at the baseline and maximum of the range of motion, this value is taken to be the more accurate of the two values. This means that Film 3 and Film 4 were inadvertently irradiated for about the same level of motion, approximately 2.5 mm. However, the remaining films exhibited the trend for the motion at the center target being larger than the motion experimentally seen at the nose. Therefore, although smaller motions yielded similar results between the two positions, discrepancies began to clearly be observed above the experimental value of 1.5 mm of motion. In fact, in the horizontal direction above 3 mm, the difference in motion between the center of the phantom and at the nose became almost twice as much.

Table 1 - Experimental (at the nose) and measured (at the center) values of the level of motion achieved by the platform in the vertical direction

<u>Film</u>	<u>Crank (mm)</u>	<u>Experimental (mm)</u>	<u>Measured (mm)</u>
1	0.025	0.5	0.5
2	0.025	1.5	1.9
3	0.025	2.0	2.6
4	0.025	3.4	2.5
5	0.025	4.0	4.7

Table 2 - Experimental (at the nose) and measured (at the center) values of the level of motion achieved by the platform in the horizontal direction

<u>Film</u>	<u>Crank (mm)</u>	<u>Experimental (mm)</u>	<u>Measured (mm)</u>
6	0.025	0.3	0.8
7	0.050	1.3	2.3
8	0.075	1.7	2.7
9	0.100	3.2	5.7
10	0.075	5.3	10.1

4.2. Absolute Dose Measurements

4.2.1 Absolute Dose Curves

Film measurements were conducted in this work as described in Section 3.8. The administered dose was 5 Gy to the center of the film, or the 100% isodose line in the target, for different levels of motion produced by the platform device in both the vertical and horizontal planes. In between each irradiation, Lucy was taken apart, a new piece of EBT3 film was reinserted before the motion was adjusted, and the irradiated film was labeled and set aside to be digitized on the following day.

The first film that was irradiated was done at a stationary, midline position and was considered the baseline and reference image during data analysis. Each film that followed was irradiated while in constant motion for the documented level as produced by the platform. Since the motion was constant during the radiation delivery, it should be noted that this was a deviation from normal patient behavior. Clinically, some of the major challenges observed during treatment delivery are situations where the patient continues to fall asleep during delivery, snore, or have a hard time holding still. Something commonly observed is the tendency for their chin to continuously drift downward in the thermoplastic mask each time. This would cause frequent interruptions of the treatment, in which another CBCT would be needed for the treatment to be continued. Even in this case, the chin motion underneath the mask is not a continuous oscillation as with the platform. Therefore, for all motion considered in this work, the results will be described for the extreme case of constant patient motion during treatment.

For each film, a total of two CBCTs were taken, one at the baseline for that particular range of motion to begin the treatment and one at the maximum displacement. This was done to later measure the motion at the film located in the center of the Lucy phantom using vector analysis between the two images. The dose given to the film from these CBCT images were taken into consideration by separately irradiating a piece of film with only one cone-beam image. After analysis, it was observed that the CBCT contributed no more than 10cGy to the overall irradiation of the film. Compared to the administered 5 Gy, or 500cGy, the contribution of the two CBCTs for each film was considered insignificant, and the subtraction was therefore omitted from the data analysis for this work.

After the film calibration was conducted as described in Section 3.9 and the irradiated test films were each digitized using the Epson11000XL scanner, data analysis began by applying the calibration to each of the films in the RIT113 dosimetry software. Once the test films were calibrated and saved, each of the target films that were irradiated during constant motion were individually compared to the reference image that was taken with no motion. This could be done because the reference film was initially analyzed and found to have received 5 Gy at the center of the film, determined by the center of the pinpricks. The geometric center of the film was within the 0.5 mm tolerance of the GK. This means that for the irradiation of the stationary target, the shifts from the CBCT were performed and the dose was delivered properly and within tolerance, which is verification that the film could be used as a baseline reference to compare to the films that were irradiated with motion. The comparison was done to observe the deviation in absolute dose and dose distribution from that administered to a stationary target. For this, the

reference image was registered to a specific target image using the pinpicks that were made on each film by the film insert cassette in the Lucy phantom, and the data was plotted for comparison in the vertical and horizontal profiles of the film. Figures 14-18 are the absolute dose curves in the vertical (red) and horizontal (green) profiles of the film for each vertical motion produced in this work, where the y-axis is the dose given in cGy and the x-axis is the position on the film given in cm. Figures 19-23 are the absolute dose curves with the same considerations for each horizontal motion.

It was expected that the film profile (vertical or horizontal) corresponding to the allowed direction of motion for each film would have the most amount of deviation from the reference curve. For example, as the vertical motion increased, the plot for the target image would be expected to have a smaller profile along the vertical profile of the film than in the horizontal, and the opposite would be true for the horizontal motion. However, since the motion of the platform was not solely a two-dimensional (2D) motion but rather a sweeping motion in each direction, this was not observed. The sweeping motion acted in the intended direction of motion but also caused additional movement both towards and away from the isocenter in each direction. Therefore, instead of the predicted motion and film profile plot correspondence, the orthogonal profiles for the larger motions in both directions showed the most deviation from the reference image. The design of the device and the convergence of the gamma radiation sources in the head of the machine interacting with the sweeping phantom motion may have been additional contributors to this deviation. Nevertheless, the unpredictable movements of the phantom made a detailed explanation for the dose distribution on the film a more complex issue. To fully understand the dose distribution, machining improvements for certain parts of

the device are needed, such as metal replacements for some of the plastic components. Additionally, multiple CT images of the device at each level of motion may be beneficial to observe the correlation of the changes in platform geometry to the changes in the range of motion.

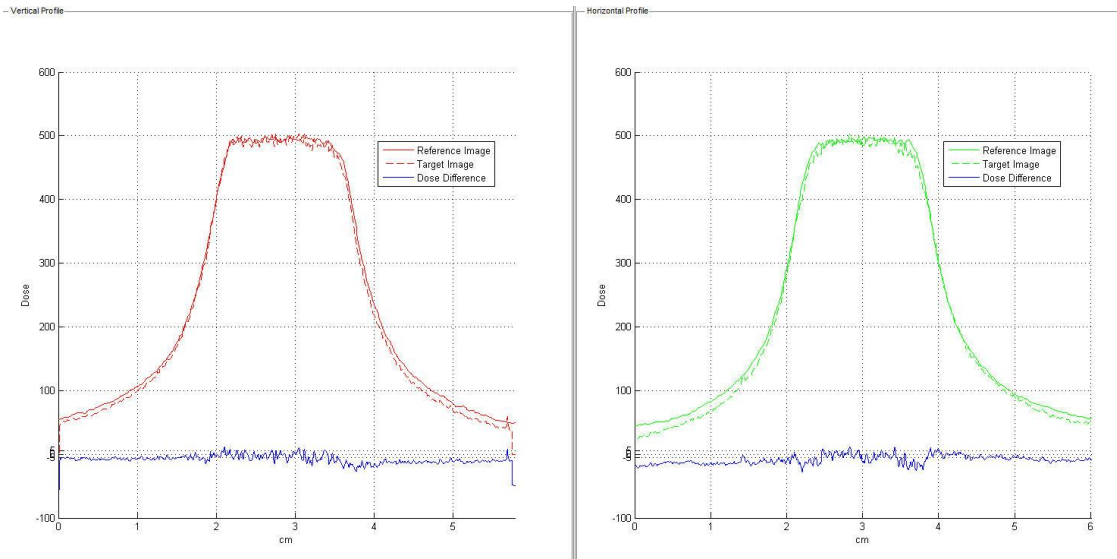


Figure 14 - Absolute dose curves in the vertical (l) and horizontal (r) profiles of Film 1, which had 0.5 mm vertical motion as observed by the IFMM, compared to the reference film with no motion. The dose along the y-axis is given in cGy and the depth (or width) along the x-axis is given in cm.

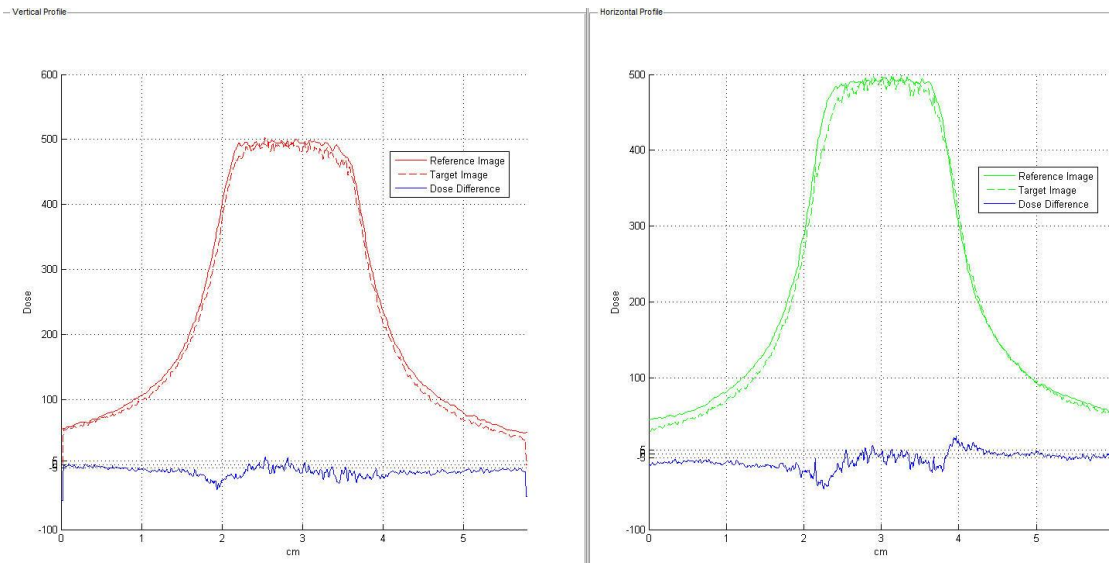


Figure 15 - Absolute dose curves in the vertical (l) and horizontal (r) profiles of Film 2, which had 1.5 mm vertical motion as observed by the IFMM, compared to the reference film with no motion. The dose along the y-axis is given in cGy and the depth (or width) along the x-axis is given in cm.

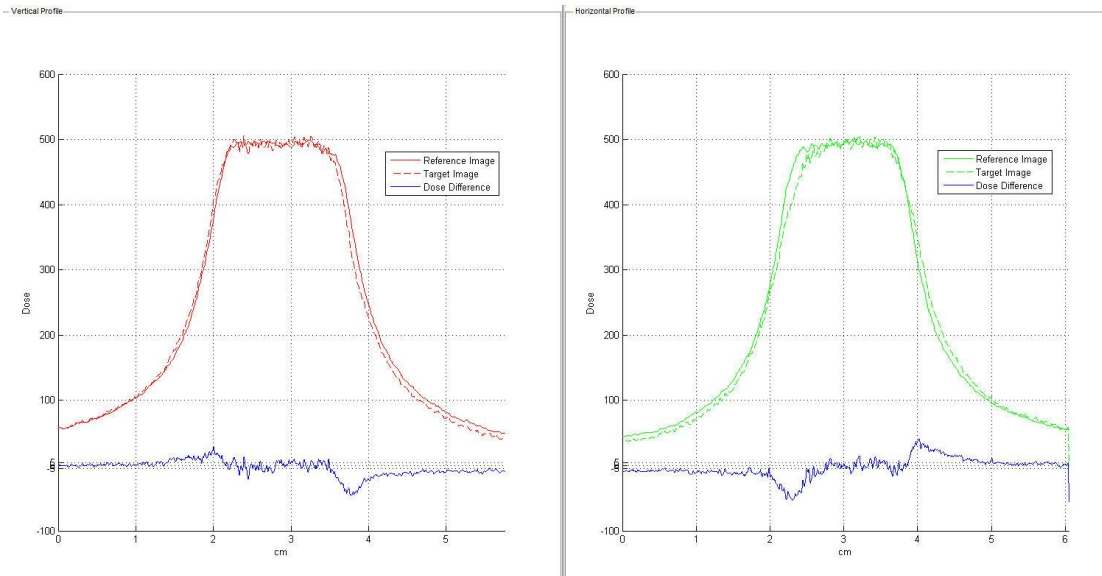


Figure 16 - Absolute dose curves in the vertical (l) and horizontal (r) profiles of Film 3, which had 2.0 mm vertical motion as observed by the IFMM, compared to the reference film with no motion. The dose along the y-axis is given in cGy and the depth (or width) along the x-axis is given in cm.

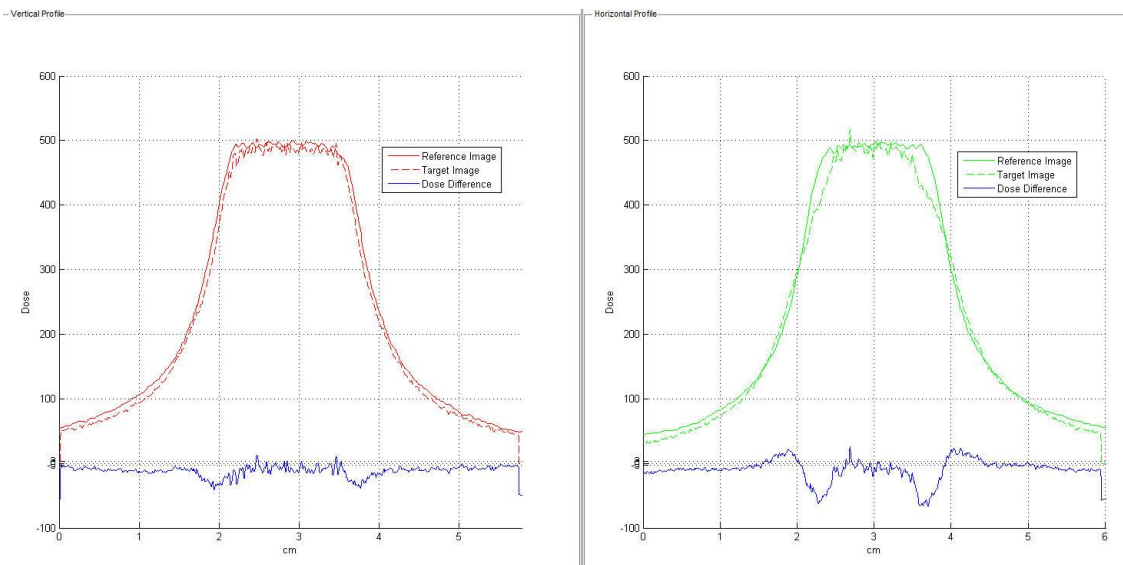


Figure 17 - Absolute dose curves in the vertical (l) and horizontal (r) profiles of Film 4, which had 3.4 mm of vertical motion as observed by the IFMM, compared to the reference film with no motion. The dose along the y-axis is given in cGy and the depth (or width) along the x-axis is given in cm.

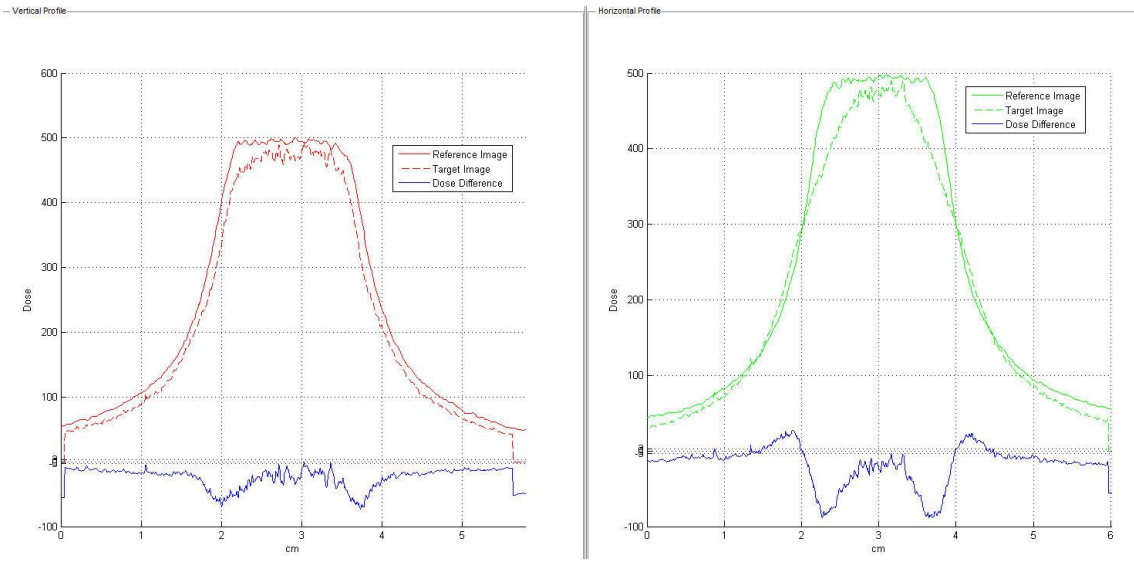


Figure 18 - Absolute dose curves in the vertical (l) and horizontal (r) profiles of Film 5, which had 4.0 mm of vertical motion as observed by the IFMM, compared to the reference film with no motion. The dose along the y-axis is given in cGy and the depth (or width) along the x-axis is given in cm.

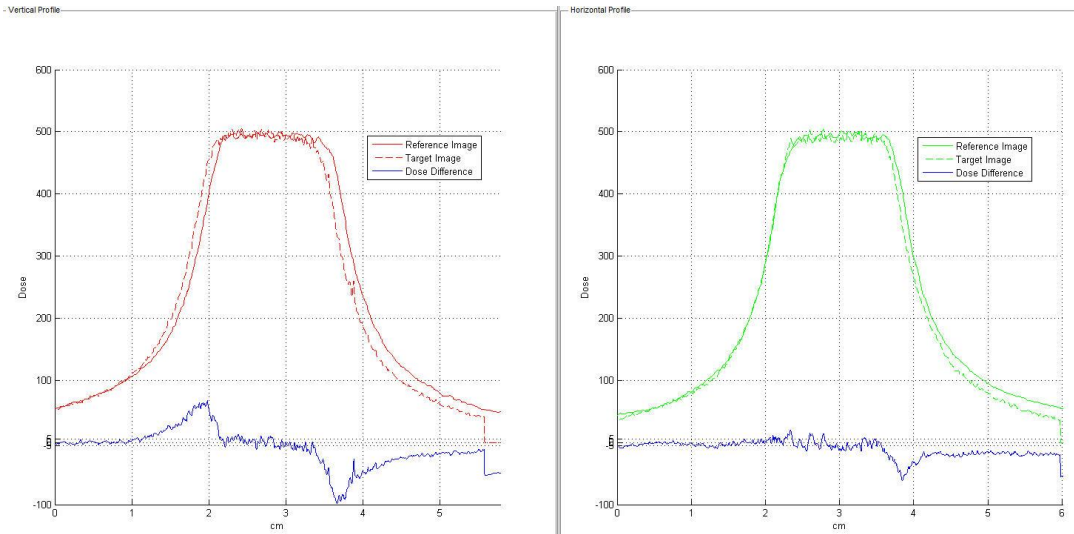


Figure 19 - Absolute dose curves in the vertical (l) and horizontal (r) profiles of Film 6, which had 0.3 mm of horizontal motion as observed by the IFMM, compared to the reference film with no motion. The dose along the y-axis is given in cGy and the depth (or width) along the x-axis is given in cm.

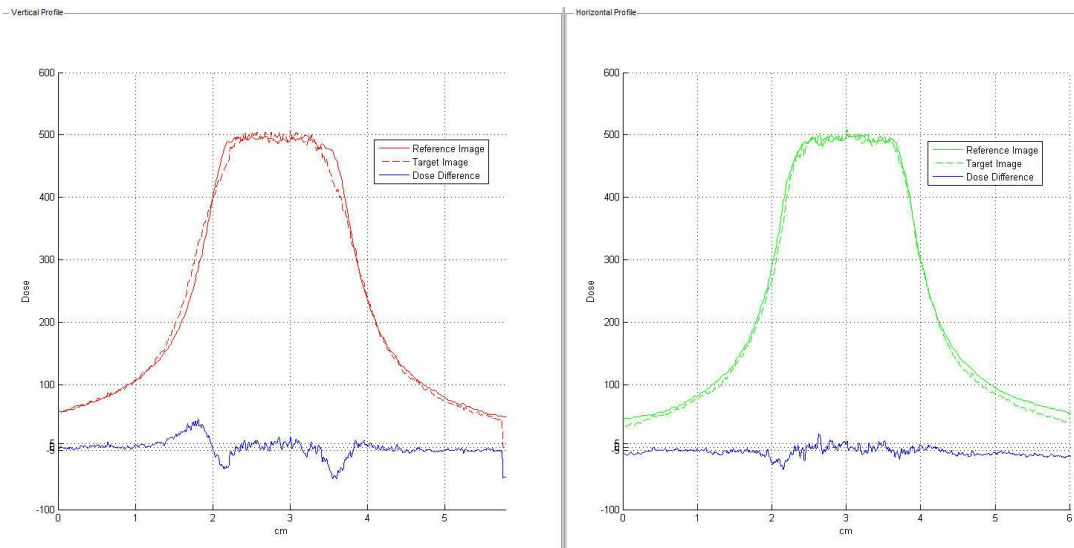


Figure 20 - Absolute dose curves in the vertical (l) and horizontal (r) profiles of Film 7, which had 1.3 mm of horizontal motion as observed by the IFMM, compared to the reference film with no motion. The dose along the y-axis is given in cGy and the depth (or width) along the x-axis is given in cm.

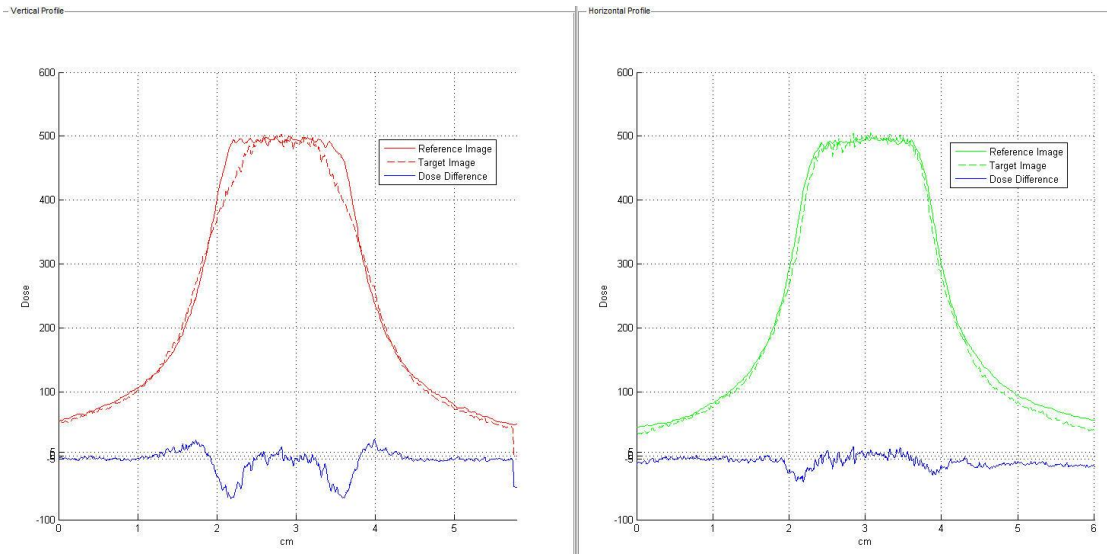


Figure 21 - Absolute dose curves in the vertical (l) and horizontal (r) profiles of Film 8, which had 1.7 mm of horizontal motion as observed by the IFMM, compared to the reference film with no motion. The dose along the y-axis is given in cGy and the depth (or width) along the x-axis is given in cm.

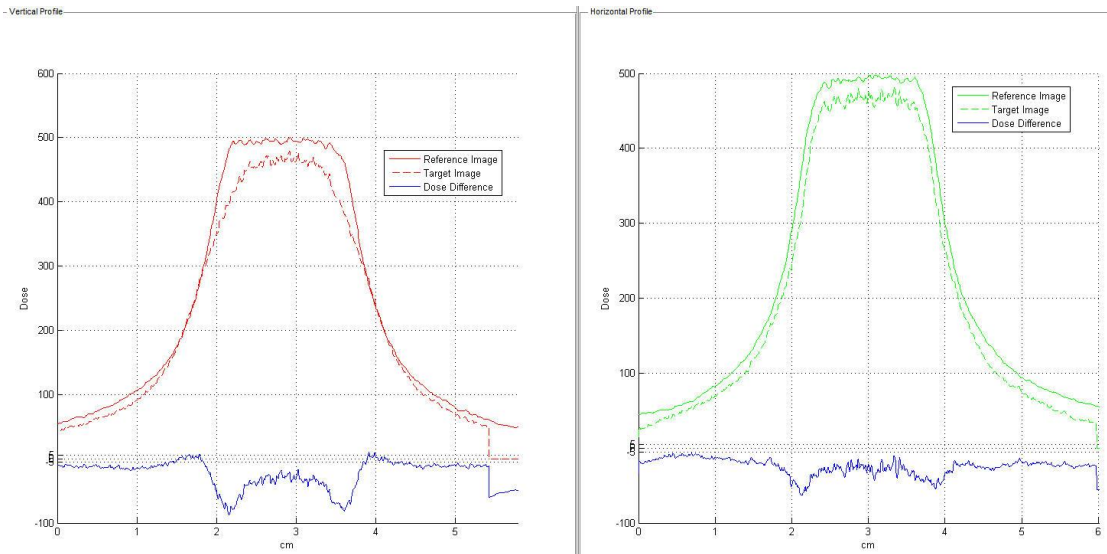


Figure 22 - Absolute dose curves in the vertical (l) and horizontal (r) profiles of Film 9, which had 3.2 mm of horizontal motion as observed by the IFMM, compared to the reference film with no motion. The dose along the y-axis is given in cGy and the depth (or width) along the x-axis is given in cm.

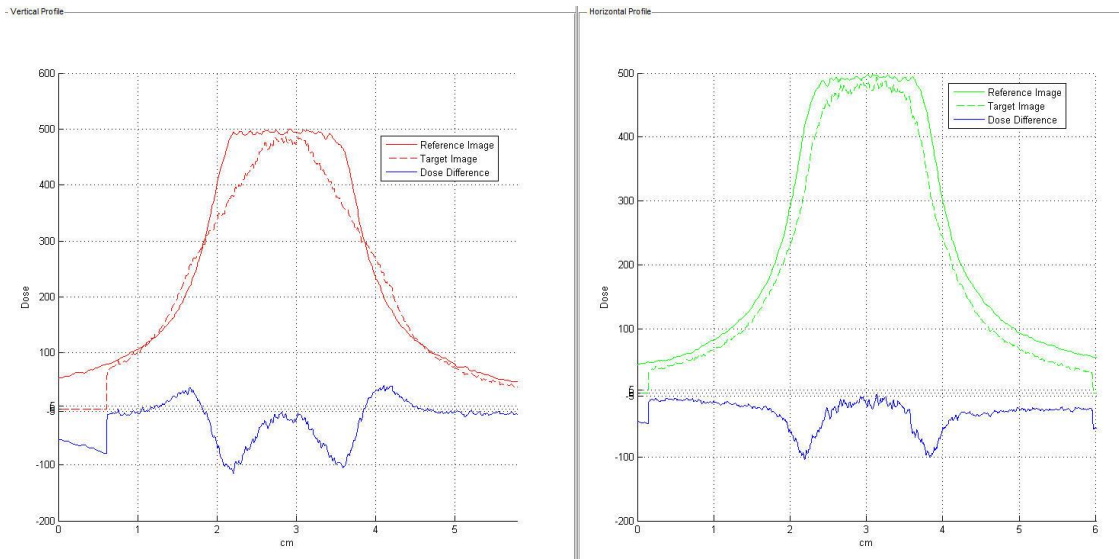


Figure 23 - Absolute dose curves in the vertical (l) and horizontal (r) profiles of Film 10, which had 5.3 mm of horizontal motion as observed by the IFMM, compared to the reference film with no motion. The dose along the y-axis is given in cGy and the depth (or width) along the x-axis is given in cm.

4.2.2 Dose Coverage for a Moving Target

As with all methods of radiation therapy, dose coverage for a target volume is an important topic and consideration during treatment planning and delivery in Gamma Knife procedures. Since GK is a radiosurgical procedure used for intracranial structures, which utilizes shots of intense gamma radiation to small targets, accuracy and coverage are highly considered in each case to give as much dose as possible to the target while keeping the dose to healthy surrounding brain tissue to a minimum. Although Elekta gives a 1.5 mm motion tolerance as measured at the nose by the IFMM system [6], it is useful to know the effects of motion on tumor coverage for different levels of motion and patient geometries.

For the extreme case of constant patient motion and nose-to-target geometry in which the tumor is situated much further from the pivot point than the nose along the horizontal plane, the absolute dose curves for vertical and horizontal motion (Figures 14-23) are considered. For a tumor approximately 1.5 cm in size, a shot of 5Gy to the center of the tumor would yield 100% coverage for a stationary target, as seen by the Reference image in all figures above. Even for motion observed at the nose as less than 2.0 mm in the corresponding film profile for both planes, full coverage would still be achievable. However, above this level, specifically above 3 mm as measured at the nose for the producible motions in this work, the percentage of tumor coverage begins to drop. A more thorough evaluation using 3D analysis would be needed to accurately give the decreases in percentage of volumetric coverage for this hypothetical tumor evaluation.

Consider the horizontal profiles of Figure 22 and Figure 23 for the same tumor, in which the tumor would not receive full coverage due to motion above 3 mm. Instead, margins around the tumor would be needed to maintain coverage, which would be a function of the size of the tumor and the amount of motion. The location of the tumor in relation to the pivot point should also be considered. As mentioned, this data was acquired using a specific geometry placing the target location further from the pivoting point than the marker at the nose. For closer tumor locations, motion would not be as much of a hindrance due to a smaller pivoting axis. Therefore, tumor coverage would remain high for large amounts of motion at the nose for closer tumors, whereas for more superior tumors, coverage would decline much quicker.

Additionally, the prescription isodose lines were considered for tumor coverage. In this work, the dose was consistently planned to the 100% isodose line at the center of the target. This corresponds to the peaks of each absolute dose curve in Figures 14-23, where deviations between the reference and target film become larger with increased motion added to the system. However, clinical gamma knife treatments are often prescribed to the 50% isodose line instead, and for more complex targets, the prescription isodose lines may vary even more. Since the dose delivered for this work was one 16 mm shot of 5 Gy, a prescription to the 50% isodose line would correspond to two shots of 2.5 Gy of radiation. Considering the same 1.5 cm tumor as before and the same plots for horizontal motion, Figure 22 and Figure 23, this would now mean that even with the large horizontal motion, there would be no loss of coverage for a 50% isodose prescription. Only the maximum dose changes were considered above; however, when

discussing motion at the tumor, the tumor coverage was shown to also depend on the prescription isodose lines used for the treatment delivery.

4.2.3 Plot Statistics

Both the differences in absolute dose and the penumbra region of the target curves when compared to the reference images were considered for the conclusions of this work. A few of the data plots had falloff regions at the edges that were caused by software interference during gamma analysis from the permanent marker used to label the films. Additionally, for larger motions as observed in Figures 22 and 23, the discrepancies at the edges of the plots were due to the amount of time it took for the phantom to move to each side of the range of motion during irradiation. This caused the dose to be widely distributed over the film and accumulate more in the regions where the most time was spent. The plot statistics given in Tables 3 and 4 took these fall-off areas into consideration and omitted them as not to hinder the most accurate information from being obtained from the corresponding absolute dose curves. The maximum and mean differences and the standard deviation values in the tables are given in cGy. For the larger motions in each plane, as in Film 5 (vertical) and Films 9 and 10 (horizontal), the maximum difference between the reference and target curves are greatest due to deviations in dose distribution caused by the increase in the level of motion being a detriment to the quality of the treatment plan delivered to the film.

Table 3 - Plot statistics corresponding to the absolute dose curves in Figures 14-18 for target films irradiated with constant vertical motion, compared to the reference film with no motion

<u>Film</u>	<u>Profile</u>	<u>Max Difference</u> <u>(cGy)</u>	<u>Mean Difference</u> <u>(cGy)</u>	<u>Std. Deviation</u> <u>(cGy)</u>
1	Vertical	27.08	7.77	5.87
	Horizontal	27.43	8.51	6.74
2	Vertical	38.46	11.38	6.80
	Horizontal	46.23	8.45	10.63
3	Vertical	26.65	3.86	5.92
	Horizontal	59.00	3.08	19.2
4	Vertical	54.70	12.26	8.8
	Horizontal	65.86	8.94	27.10
5	Vertical	72.74	19.77	16.91
	Horizontal	88.56	13.75	27.05

Table 4 - Plot statistics corresponding to the absolute dose curves in Figures 19-23 for target films irradiated with constant horizontal motion, compared to the reference film with no motion

<u>Film</u>	<u>Profile</u>	<u>Max Difference</u> <u>(cGy)</u>	<u>Mean Difference</u> <u>(cGy)</u>	<u>Std. Deviation</u> <u>(cGy)</u>
6	Vertical	98.12	7.68	29.13
	Horizontal	58.17	9.68	12.23
7	Vertical	50.39	0.95	13.71
	Horizontal	21.62	7.48	6.95
8	Vertical	67.69	7.80	18.09
	Horizontal	40.86	9.40	8.57
9	Vertical	87.42	21.67	20.99
	Horizontal	62.77	24.71	10.81
10	Vertical	114.53	17.73	36.98
	Horizontal	104.45	31.02	21.71

CHAPTER 5. CONCLUSION

When considering the movement of an intracranial tumor during treatment on the Leksell Gamma Knife Icon system, it is inaccurate to simply state that the movements are either less than or equal to the movements at the nose of a patient as observed by the motion management system. Instead, the patient geometry, which considers the location of the tumor in relation to both the nose and the pivoting point at the C1 vertebra, should be accounted for as well.

With the use of a stereotactic QA phantom, GAFChromic film placed at the center of this phantom, and a platform device that produced constant patient-like chin movements, it was shown that motion at a tumor could be much greater than what is observed by the motion management system. Realistically, a patient would not be able to be treated with the GK while moving more than 3 mm, where this deviation was observed, and constant patient motion is also not a concern for this treatment. However, depending on the location of the tumor, readings of the HDMM may not correlate with a smaller movement at the tumor. By primary evaluation, it can be stated that more superior tumors can have greater movement during treatment than what is observed and predicted by the white paper documentation of the IFMM system. Not only should the location of the tumor in the skull be considered but also the location of the tumor in relation to the nose and pivot point at the neck of the patient as well. Additionally, when discussing tumor coverage for a moving target or a particularly fidgety patient, the prescription isodose line may play a key factor in the quality of the treatment delivery.

To further evaluate these findings in the future, the platform device could be modified to perform more stable movements. These modifications may include an upgrade to a metal driving linkage and metal adjustment screws, which would rid the setup of any extra motion between oscillations and make the IFMM readings more stable between each level of motion. This would also allow the step sizes of the levels of motion to be chosen more clearly and observed more accurately. The position of the driving linkage connection with the pivoting frame could also be placed in a more stabilizing location for each direction. For example, the linkage position for the vertical direction could be centered at the top or bottom of the frame to produce a cleaner motion, and the position for the horizontal motion could be moved to one of the sides of the frame instead. This would cut down any additional torqueing of the pivoting frame that may cause discrepancies in the dose delivery. Additionally, to refine the testing and prevent the extreme case of continuous motion during irradiation, a motor controller for the platform could be programmed to exhibit the actual movements of a patient as read by the IFMM during heightened points of movement in an actual treatment.

The incorporation of the integrated CBCT and IFMM systems has provided a more comfortable treatment option for Gamma Knife patients. However, before new treatments can be conducted with the Leksell Gamma Knife Icon, all system upgrades and modifications should be properly tested for every potential clinical situation. Patients count on the therapeutic devices that administer their treatments to provide them the best possible outcome as described by their function, which is communicated to the patient by the radiation team. However, it is the job of the medical physicist, specifically, to ensure that each patient receives the best treatment possible. This includes the production and

approval of optimized treatment plans and the assurance that the plans are delivered in the most accurate way possible. As technology continues to progress and treatment machines become more complex, a continued effort must be made to understand and investigate their methodology, as well as to consider the physical additions that accompany them.

REFERENCES

- [1] Almond, Peter, et al. "AAPM's TG-51 Protocol for Clinical Reference Dosimetry of High-Energy Photon and Electron Beams." *Medical Physics* 26 (1999): 1847-1870. doi:10.1118/1.598691.

- [2] Chung, C, et al. "Clinical Evaluation of a Novel Thermoplastic Mask System with Intrafraction Motion Monitoring using IR Tracking and Cone-beam CT for Gamma Knife Radiosurgery". ASTRO Presentation. San Francisco, 2014. Poster.

- [3] DeWerd, Larry, et al. "Ionization Chamber Instrumentation." Ed. University of Wisconsin. Madison, WI: AAPM, n.d. PowerPoint.

- [4] Elekta. "High Definition Motion Management - Enabling Stereotactic Gamma Knife Radiosurgery with Non-Rigid Patient Fixations". Stockholm, Sweden: Elekta Instrument AB, 2015. Document.

- [5] Elekta.com. Leksell Gamma Knife Icon. 2017. Web.

- [6] Elekta. "Leksell Gamma Knife Icon: Instructions for Use". Manual. Stockholm, Sweden: Elekta Instrument AB., 2015. Document.

- [7] Elekta. "Leksell GammaPlan: Online Reference Manual". Manual. Stockholm, Sweden: Elekta Instrument AB, 2015. Document .

- [8] GAFChromic.com. "Efficient Protocols for Accurate Radiochromic Film Calibration and Dosimetry." Manual. Document.

- [9] GAFChromic.com. "GAFChromic Dosimetry Media, Type EBT-3." Specification.

- [10] Giles, Matthew. Masters Thesis Notebook.

- [11] Li, Winnie, et al. "Preliminary Evaluation of a Novel Thermoplastic Mask System with Intrafraction Motion Monitoring for Future Use with Image-Guided Gamma Knife." *Cureus Journal of Medical Science* v.8(3) (2016).
- [12] McDonald, Daniel, et al. "Calibration of the Gamma Knife Perfexion using TG-21 and the Solid Water Leksell Dosimetry Phantom." *Medical Physics* 38 (2011): 1685-1693. doi: 10.1118/1.3557884.
- [13] University of Virginia School of Medicine. History and Technical Overview of the Gamma Knife. 2017. Web.
- [14] Meltsner, Sheridan and Larry DeWerd. "Air Kerma Based Dosimetry Calibration for the Leksell Gamma Knife." *Medical Physics* 36(2) (2009): 339-350.
- [15] Mutic, Sasa, et al. "Quality Assurance for Computed-Tomography Simulators and the Comuted Tomography Simulation Process: Report of the AAPM Radiation Therapy Comittee Task Group No. 66." *Medical Physics* 30(10) (2003): 2762-2792. doi: 10.1118/1.1609271.
- [16] Schulz, Robert, et al. "A Protocol for the Determination of Absorbed Dose from High-Energy Photon and Electron Beams: Task Group 21." *Medical Physics* 10(6) (1983): 741-771.
- [17] Standard Imaging, Inc. Lucy 3D QA Phantom REF 91210. Manual. Middleton, WI: Standard Imaging, Inc., 2017. Document.